Higher-Order Derivatives of the Kinematic and Dynamic Equations for Dynamic Synthesis of a Watt-II Six-Bar Linkage

Jacob P. Meijaard and Volkert van der Wijk

Abstract For the purpose of dynamic synthesis, an efficient procedure for computing higher-order time derivatives of the kinematic and dynamic equations of mechanisms with rigid links is presented. It is based on a finite-element modelling of the mechanism, in which the rigidity is imposed by prescribing zero discrete deformations as constraints. Choosing simple expressions for the deformations and a constant mass matrix of the elements makes the computations efficient. The procedure is used for the dynamic synthesis of a Watt type-II six-bar linkage. For a constant vertical load in the output point, an approximately constant horizontal velocity of this point near a working point and a zero driving torque, the mass parameters of the links are derived. A number of time derivatives is set to zero, which yields equations that are linear in the chosen mass parameters. Simulations show the nearly constant velocity over a range of motion.

1 Introduction

Contrary to designing a mechanism in the conventional way by dynamic analysis, where the desired dynamic properties are obtained with an iterative optimization of the design, dynamic synthesis has the purpose to derive the design of a mechanism directly from the desired dynamic properties. For some dynamic properties, it is necessary to have higher-order derivatives of the kinematic and dynamic equations available.

J. P. Meijaard
Delft University of Technology, Delft, The Netherlands
e-mail: j.p.meijaard@tudelft.nl

V. van der Wijk
Kinetic Art Sculptures, The Netherlands
e-mail: Volkert.vanderWijk@kineticart.nl

In the kinematic and dynamic analysis of a mechanism consisting of rigid links, first the positions and orientations have to be determined from the values of the degrees of freedom. Then, the velocities and angular velocities of the bodies for the found configuration have to be determined for given values of the rates of the degrees of freedom. For kinematically driven mechanisms, higher-order time derivatives can be obtained from given values of the higher-order time derivatives of the degrees of freedom, for which derivatives up to a certain order of the kinematic constraint equations have to be determined and analysed. For dynamically driven mechanisms, the second time derivatives, the accelerations, of the degrees of freedom are determined from the equations of motion. For higher-order derivatives, the equations of motion have to be differentiated.

Higher-order time derivatives for the kinematics and dynamics have several applications, such as the design or approximation of a path, the numerical integration of the equations of motion [1], the inverse dynamics [2], the design of controllers and the design for dynamics, such as the dynamic balancing of mechanisms. Müller and Kumar [3] used screw theory and Lie algebra to calculate derivatives of the equations of motion up to the second order. This paper shows their use in the synthesis of the mass distribution of a Watt type-II six-bar linkage to achieve a desired dynamic task: the mechanism has to support a vertical load at the output point and simultaneously has to have an approximately constant horizontal velocity under a zero driving torque.

2 Time derivatives of the kinematic equations

In the finite element description of a multibody dynamic system used here, the nodal coordinates $\boldsymbol{x}$ are related to generalized strains $\boldsymbol{\varepsilon}$ by deformation functions $\boldsymbol{D}$ as

$$\boldsymbol{\varepsilon} = \boldsymbol{D}(\boldsymbol{x}). \tag{1}$$

For instance, the deformation of a truss element, described by two nodes at its ends, having the node numbers p with the coordinates $(x^p, y^p, z^p)^{\mathrm{T}}$ and q with the coordinates $(x^q, y^q, z^q)^{\mathrm{T}}$, can be defined as [4]

$$\varepsilon_1 = \frac{l^2 - l_0^2}{2l_0} = \frac{(x^q - x^p)^2 + (y^q - y^p)^2 + (z^q - z^p)^2 - l_0^2}{2l_0}, \tag{2}$$

where l_0 is the undeformed length of the truss element and l is its current length.

Rigid elements can be defined by equating the generalized strains to zero, $\boldsymbol{\varepsilon} = \boldsymbol{0}$, which is the case we consider here. The coordinates that do not have prescribed values can be partitioned into independent coordinates, $\boldsymbol{x}^{\mathrm{d}}$, and dependent coordinates, $\boldsymbol{x}^{\mathrm{c}}$. The number of dependent coordinates is equal to the number of deformation functions. For current values of the independent coordinates, the dependent coordinates can be solved from Eq. (1), for instance by a Newton–Raphson iteration: if Eq. (1) is not satisfied for approximate values of the dependent coordinates, $\boldsymbol{x}^{\mathrm{c}}$, increments are found from

$$\boldsymbol{D}_{,\boldsymbol{x}^{\mathrm{c}}} \Delta\boldsymbol{x}^{\mathrm{c}} = -\boldsymbol{D}, \tag{3}$$

where a subscript comma followed by variables denotes partial derivatives with respect to these variables. From the solution, a new estimate of the dependent variables is obtained as $\boldsymbol{x}^{\mathrm{c}} + \Delta\boldsymbol{x}^{\mathrm{c}}$. The procedure is repeated until sufficiently accurate values of the dependent coordinates are obtained.

By taking a time derivative of Eq. (1), we obtain

$$\dot{\boldsymbol{\varepsilon}} = \boldsymbol{0} = \boldsymbol{D}_{,\boldsymbol{x}^{\mathrm{c}}} \dot{\boldsymbol{x}}^{\mathrm{c}} + \boldsymbol{D}_{,\boldsymbol{x}^{\mathrm{d}}} \dot{\boldsymbol{x}}^{\mathrm{d}}, \tag{4}$$

from which the dependent velocities can be solved and expressed in the coordinates and the independent velocities as

$$\dot{\boldsymbol{x}}^{\mathrm{c}} = -\left(\boldsymbol{D}_{,\boldsymbol{x}^{\mathrm{c}}}\right)^{-1} \boldsymbol{D}_{,\boldsymbol{x}^{\mathrm{d}}} \dot{\boldsymbol{x}}^{\mathrm{d}} = \boldsymbol{X}^{\mathrm{c}} \dot{\boldsymbol{x}}^{\mathrm{d}}, \quad \boldsymbol{X}^{\mathrm{c}} = -\left(\boldsymbol{D}_{,\boldsymbol{x}^{\mathrm{c}}}\right)^{-1} \boldsymbol{D}_{,\boldsymbol{x}^{\mathrm{d}}}. \tag{5}$$

Here, $\boldsymbol{X}^{\mathrm{c}}$ is the first-order transfer function for the dependent coordinates, which are the derivatives of the dependent velocities with respect to the independent velocities. Taking another time derivative of Eq. (4) yields

$$\ddot{\boldsymbol{\varepsilon}} = \boldsymbol{0} = \boldsymbol{D}_{,\boldsymbol{x}^{\mathrm{c}}} \ddot{\boldsymbol{x}}^{\mathrm{c}} + \boldsymbol{D}_{,\boldsymbol{x}^{\mathrm{d}}} \ddot{\boldsymbol{x}}^{\mathrm{d}} + (\boldsymbol{D}_{,\boldsymbol{x}\boldsymbol{x}} \dot{\boldsymbol{x}}) \dot{\boldsymbol{x}}, \tag{6}$$

from which the dependent accelerations can be expressed in the coordinates and the independent velocities and accelerations as

$$\ddot{\boldsymbol{x}}^{\mathrm{c}} = \boldsymbol{X}^{\mathrm{c}} \ddot{\boldsymbol{x}}^{\mathrm{d}} - \left(\boldsymbol{D}_{,\boldsymbol{x}^{\mathrm{c}}}\right)^{-1} \left[(\boldsymbol{D}_{,\boldsymbol{x}\boldsymbol{x}} \dot{\boldsymbol{x}}) \dot{\boldsymbol{x}}\right]. \tag{7}$$

Higher-order time derivatives of the dependent coordinates can be expressed in terms of time derivatives of the independent coordinates by subsequent differentiations of the deformation functions. In index notation, we use lower-case Latin indices for both the generalized strains and the dependent coordinates, which have the same number of components, lower-case Greek indices for the independent coordinates and upper-case Latin indices for all coordinates. Derivatives with respect to coordinates will be indicated by a comma followed by the indices of these coordinates. Time derivatives of a higher order than the second are denoted by a superscript number between parentheses indicating the order. Taking time derivatives of the deformation functions yields

$$D_{i,j} \ddot{x}_j + D_{i,\alpha} \ddot{x}_\alpha + D_{i,JK} \dot{x}_J \dot{x}_K = 0, \tag{8}$$

$$D_{i,j} x_j^{(3)} + D_{i,\alpha} x_\alpha^{(3)} + 3 D_{i,JK} \dot{x}_J \ddot{x}_K + D_{i,JKL} \dot{x}_J \dot{x}_K \dot{x}_L = 0, \tag{9}$$

$$D_{i,j}x_j^{(4)} + D_{i,\alpha}x_\alpha^{(4)} + D_{i,JK}(4\dot{x}_J x_K^{(3)} + 3\ddot{x}_J\ddot{x}_K) + 6D_{i,JKL}\dot{x}_J\dot{x}_K\ddot{x}_L + D_{i,JKLM}\dot{x}_J\dot{x}_K\dot{x}_L\dot{x}_M = 0, \tag{10}$$

$$D_{i,j}x_j^{(5)} + D_{i,\alpha}x_\alpha^{(5)} + D_{i,JK}(5\dot{x}_J x_K^{(4)} + 10\ddot{x}_J x_K^{(3)}) + D_{i,JKL}(10\dot{x}_J\dot{x}_K x_L^{(3)} + 15\dot{x}_J\ddot{x}_K\ddot{x}_L) + 10D_{i,JKLM}\dot{x}_J\dot{x}_K\dot{x}_L\ddot{x}_M + D_{i,JKLMN}\dot{x}_J\dot{x}_K\dot{x}_L\dot{x}_M\dot{x}_N = 0, \tag{11}$$

The dependent time derivatives can be expressed in the time derivatives of the degrees of freedom by solving the equations in sequence. Further time derivatives can be obtained from subsequent derivatives.

3 Equations of motion and their time derivatives

Each element gives a contribution to the mass matrix, possibly depending on its configuration, a vector containing inertia terms that are quadratic in the velocities and force terms, for instance, terms due to gravity. Also the nodes can give contributions due to lumped masses and applied forces and moments. These terms are collected in a global mass matrix, $\boldsymbol{M}$, a vector of inertia terms quadratic in the velocities, $\boldsymbol{h}$, and a force vector, $\boldsymbol{f}$. With the transpose of the first-order transfer function, $\boldsymbol{X}^{\mathrm{T}} = [\boldsymbol{X}^{c\mathrm{T}}\boldsymbol{I}]$, the equations of motion can be written as

$$\boldsymbol{X}^{\mathrm{T}}(\boldsymbol{M}\ddot{\boldsymbol{x}} + \boldsymbol{h}) = \boldsymbol{X}^{\mathrm{T}}\boldsymbol{f}, \tag{12}$$

where the accelerations have to be written in terms of the independent accelerations and the velocities and coordinates. After solving these equations for the independent accelerations, the dependent accelerations can be obtained from Eq. (7).

Time derivatives of the first-order transfer functions can be obtained by taking derivatives from the equation for these transfer functions,

$$D_{i,j}X_{j,\alpha} + D_{i,\alpha} = 0. \tag{13}$$

Time derivatives yield

$$D_{i,j}\dot{X}_{j,\alpha} + D_{i,JK}X_{J,\alpha}\dot{x}_K = 0, \tag{14}$$

$$D_{i,j}\ddot{X}_{j,\alpha} + D_{i,JK}(2\dot{X}_{J,\alpha}\dot{x}_K + X_{J,\alpha}\ddot{x}_K) + D_{i,JKL}X_{J,\alpha}\dot{x}_K\dot{x}_L = 0, \tag{15}$$

$$\begin{aligned} D_{i,j} X^{(3)}_{j,\alpha} + D_{i,JK}(3\ddot{X}_{J,\alpha}\dot{x}_K + 3\dot{X}_{J,\alpha}\ddot{x}_K + X_{J,\alpha}x^{(3)}_K) \\ + D_{i,JKL}(3\dot{X}_{J,\alpha}\dot{x}_K\dot{x}_L + 3X_{J,\alpha}\dot{x}_K\ddot{x}_L) \\ + D_{i,JKLM}X_{J,\alpha}\dot{x}_K\dot{x}_L\dot{x}_M = 0, \end{aligned} \tag{16}$$

Higher-order derivatives of the first-order transfer function can be obtained from subsequent differentiations. Elements having simple deformation functions make this computation efficient and the expressions manageable.

Higher-order time derivatives can be obtained from time derivatives of the equations of motion. The mass matrix should be ideally constant and the velocity terms should vanish, so their derivatives are zero. To a large extent, this can be achieved by modelling systems for the largest part with truss elements with quadratic deformation functions and constant mass matrices as shown in [5].

For the case of a constant mass matrix and no velocity-dependent inertia terms, the equations of motion and their time derivatives become

$$X_{I,\alpha}M_{IJ}\ddot{x}_J = X_{I,\alpha}f_I, \tag{17}$$

$$X_{I,\alpha}M_{IJ}x^{(3)}_J + \dot{X}_{I,\alpha}M_{IJ}\ddot{x}_J = X_{I,\alpha}\dot{f}_I + \dot{X}_{I,\alpha}f_I, \tag{18}$$

$$\begin{aligned} X_{I,\alpha}M_{IJ}x^{(4)}_J + 2\dot{X}_{I,\alpha}M_{IJ}x^{(3)}_J + \ddot{X}_{I,\alpha}M_{IJ}\ddot{x}_J \\ = X_{I,\alpha}\ddot{f}_I + 2\dot{X}_{I,\alpha}\dot{f}_I + \ddot{X}_{I,\alpha}f_I, \end{aligned} \tag{19}$$

$$\begin{aligned} X_{I,\alpha}M_{IJ}x^{(5)}_J + 3\dot{X}_{I,\alpha}M_{IJ}x^{(4)}_J + 3\ddot{X}_{I,\alpha}M_{IJ}x^{(3)}_J + X^{(3)}_{I,\alpha}M_{IJ}\ddot{x}_J \\ = X_{I,\alpha}f^{(3)}_I + 3\dot{X}_{I,\alpha}\ddot{f}_I + 3\ddot{X}_{I,\alpha}\dot{f}_I + X^{(3)}_{I,\alpha}f_I, \end{aligned} \tag{20}$$

The process of differentiating can be continued to yield higher-order derivatives.

4 Dynamic Synthesis of a Watt-II Six-Bar Linkage

A Watt type-II six-bar linkage is shown in Figure 1. The linkage is driven at link 1 by a torque dual to the angle θ_1 and the lengths of the links are given as in Table 1. For dynamic synthesis, here the lengths e_i and f_i, the masses m_i and the moments of inertia I_i about the centres of mass S_i $(i = 1, 2, 3, 4, 5)$ have to be determined from a desired dynamic input and output.

Table 1 Link lengths of the Watt type-II linkage.

$l_1 = 330$ mm,	$l_2 = 720$ mm,	$l_3 = 480$ mm,	$l_4 = 510$ mm,	$l_5 = 450$ mm,
$l_6 = 604.67$ mm,	$l_7 = 375$ mm,	$l_8 = 545.18$ mm,	$l_9 = 450$ mm,	$l_{10} = 1440$ mm

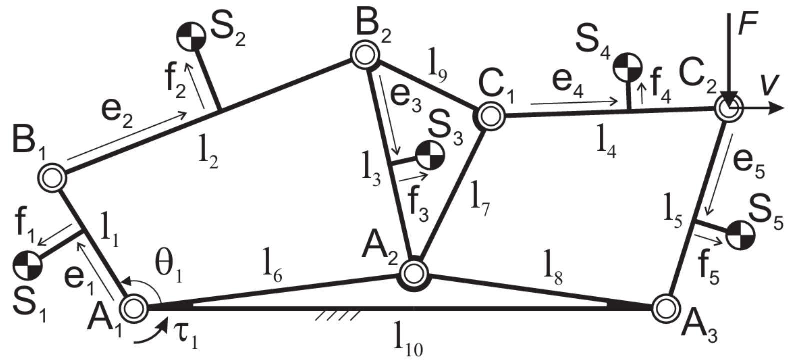

Fig. 1 Watt type-II six-bar linkage

The coordinates consist of the horizontal and vertical positions of the seven joints and the angle of the driven link θ_1. Six coordinates of the grounded joints are fixed, so there are nine free coordinates. The deformation functions for the seven moving links are given as in Eq. (2) with all z-coordinates equal to zero. For the driven link, an additional constraint is formulated for the relation between the driven angle and the coordinates as

$$\varepsilon_1 = -(x^q - x^p)\sin\theta_1 + (y^q - y^p)\cos\theta_1 = 0. \tag{21}$$

The chosen degree of freedom is the link angle θ_1 for simulations and the horizontal coordinate of the output point C_2 for the design.

The mass matrix of the links is represented as [6]

$$\boldsymbol{M}_i = \begin{bmatrix} M_{i,11} & 0 & M_{i,13} & M_{i,14} \\ 0 & M_{i,11} & -M_{i,14} & M_{i,13} \\ M_{i,13} & -M_{i,14} & M_{i,33} & 0 \\ M_{i,14} & M_{i,13} & 0 & M_{i,33} \end{bmatrix} \tag{22}$$

with

$$\begin{aligned} M_{i,11} &= [I_i + m_i((l_i - e_i)^2 + f_i^2)]/l_i^2, \\ M_{i,13} &= -[I_i + m_i f_i^2 - m_i e_i(l_i - e_i)]/l_i^2, \\ M_{i,14} &= -m_i f_i/l_i, \\ M_{i,33} &= [I_i + m_i(e_i^2 + f_i^2)]/l_i^2. \end{aligned} \tag{23}$$

The mass of the links connected to the ground only appears in the equations of motion as a moment of inertia with respect to the grounded joint, which can be replaced by a single point mass at the other joint, which in turn can be absorbed in the mass matrices of the two coupler links 2 and 4. Since each link has four independent mass parameters, the two couplers give eight mass parameters. Because mass can be redistributed between the joints B_2 and C_1, only seven of these parameters are independent. The relations (23) can be inverted for the physical parameters as

$$
\begin{aligned}
m_i &= M_{i,11} + M_{i,33} + 2M_{i,13}, \\
f_i &= -M_{i,14} l_i / m_i, \\
e_i &= l_i (M_{i,13} + M_{i,33}) / m_i, \\
I_i &= l_i^2 M_{i,11} - m_i((l_i - e_i)^2 + f_i^2).
\end{aligned} \tag{24}
$$

A part of the mass can be split off and put in the links connected to the ground.

As an example, the dynamic synthesis is shown where the output point C_2 moves at a constant horizontal velocity v under a constant vertical load F at the same point for a constant zero driving torque at the input link. In the working point, the point C_2 has a horizontal distance of 1.2 m from the point A_1. The solution is approximated by setting as many time derivatives of the velocity as possible to zero through appropriate choice of the mass parameters. For the six-bar mechanism, seven independent mass parameters are available, so at most seven time derivatives of the velocity can be prescribed. Since forces are proportional to the mass and the square of the velocity, the prescribed force and velocity can be normalized to unity: 1 N downward and 1 m/s to the right. The solution for different forces and velocities can then be found by scaling the masses proportionally to FL/v^2, where L is a characteristic length scale. The moments of inertia scale proportionally to FL^3/v^2.

Setting the time derivatives of the degree of freedom to their desired values and determining the dependent derivatives through the kinematic equations, the equations of motion and their derivatives (17)–(20) yield linear equations in the seven mass parameters to be determined. The total calculation time for setting up the equations and solving them is less than 0.05 s on a standard laptop computer. It appears to be impossible to find a feasible mass distribution if all seven conditions on the derivatives of v are imposed; some mass values and moments of inertia become negative. So only four derivatives of the velocity are required to be zero. This allows us to choose a mass distribution for link 2 and to determine the four mass parameters of link 4 from the four linear equations. The chosen and computed physical mass parameters for this example are shown in the upper part of Table 2. Note that most of the mass is assigned to link 4. As e_4 is larger than l_4, the centre of mass is to the right of the point C_2. The masses of the links 1, 3 and 5 are zero in the calculations, because their masses are absorbed in those of the links 2 and 4. For a real design, a part of the mass can be redistributed to give all links a positive mass, while the dynamics remains the same. As a possible example of this redistribution, the mass parameters as in the lower part of Table 2 are chosen.

On the basis of this mass distribution, the motion of the mechanism has been simulated in the multibody program Spacar [7]. Figure 2 shows the horizontal position of the output point C_2 and the horizontal velocity of the same point as functions of the time. The motion is periodic with a period of

Table 2 Mass properties of the links for the numerical example

$m_2 = 0.00105$ kg,	$I_2 = 24.686$ kg mm^2,	$e_2 = 685.714$ mm,	$f_2 = 0$ mm
$m_4 = 0.56559$ kg,	$I_4 = 928.219$ kg mm^2,	$e_4 = 860.597$ mm,	$f_4 = -119.673$ mm
$m_1 = 0.000025$ kg,	$I_1 = 2.226$ kg mm^2,	$e_1 = 132$ mm,	$f_1 = 49.5$ mm
$m_2 = 0.000525$ kg,	$I_2 = 12.343$ kg mm^2,	$e_2 = 685.714$ mm,	$f_2 = 0$ mm
$m_3 = 0.0005$ kg,	$I_3 = 94.176$ kg mm^2,	$e_3 = 288$ mm,	$f_3 = 72$ mm
$m_4 = 0.56459$ kg,	$I_4 = 790.736$ kg mm^2,	$e_4 = 861.218$ mm,	$f_4 = -119.885$ mm,
$m_5 = 0.001$ kg,	$I_5 = 165.544$ kg mm^2	$e_5 = 270$ mm,	$f_5 = 67.5$ mm

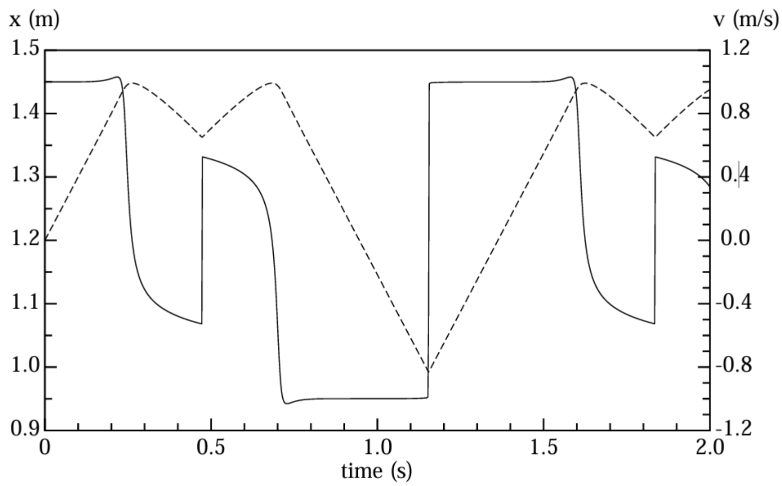

Fig. 2 Horizontal position of the point C_2 (dashed, left scale) and its horizontal velocity (fully drawn, right scale)

1.363 s. In each period, there are two time intervals in which the velocity is nearly constant, one with a negative velocity and one with a positive velocity. There are two maxima in each period, corresponding to the configurations in which the links 7 and 4 are aligned. At the time 1.155 s, at the minimum in which the links 1 and 2 are aligned, a peak in the acceleration occurs and the velocity is reversed. The high acceleration is due to the large difference in mass of the links 2 and 4. The velocity as a function of time shows more clearly the approximately constant value of the velocity in two intervals and the sharp jump in the velocity between them. Although in this example the link lengths are chosen, in general they can also be considered free to derive for dynamic synthesis, enabling optimization of the design.

5 Conclusions

We have shown an efficient procedure based on a finite element formulation for computing the time derivative of the kinematic and dynamic equations of planar linkages with rigid links. The efficiency is due to the derivation procedure, the simple form of the constraint equations and the constant mass matrices of the links. The time derivatives of the equation of motion of a Watt type-II six-bar linkage were used as an example for dynamic synthesis, to obtain the mass distribution which yields an approximately constant velocity of the output point under a constant external force and a zero driving torque. The calculation times are so short that a reliable comparison with other methods is not possible. As the procedure is presented in a general form, applications beyond planar rigid linkages to systems with several degrees of freedom, spatial systems and systems containing flexible links are possible.

References

1. Milenkovic, P.: Solution of the forward dynamics of a single-loop linkage using power series. ASME J. Dyn. Sys. Meas. Control 133, 061002-1–9 (2011).
2. Höpler, R., Thümmel, M.: Symbolic computation of the inverse dynamics of elastic joint robots. In: Proceedings of the 2004 IEEE International Conference on Robotics and Automation, vol. 5, pp. 4314–4319. IEEE, Piscataway NJ, (2004).
3. Müller, A., Kumar, S.: Closed-form time derivatives of the equations of motion of rigid body systems. Multibody Syst. Dyn. 53, 257–273 (2021).
4. Besseling, J.F.: Non-linear theory for elastic beams and rods and its finite element representation, Comp. Meth. Appl. Mech. Eng. 31, 205–220 (1982).
5. Meijaard, J.P.: Modelling rigid and flexible bodies with truss elements. In: Kecskeméthy, A., Geu Flores, F. (eds.) Multibody Dynamics 2019, Proceedings of the 9th ECCOMAS Thematic Conference on Multibody Dynamics, pp. 275–282. Springer Nature Switzerland, Cham, (2020).
6. Meijaard, J.P., van der Wijk, V.: Principal vectors and equivalent mass descriptions for the equations of motion of planar four-bar mechanisms, Multibody Syst. Dyn. 48, 259–282 (2020).
7. Jonker, J.B., Meijaard, J.P.: SPACAR – Computer program for dynamic analysis of flexible spatial mechanisms and manipulators. In: Schiehlen, W. (ed.) Multibody Systems Handbook, pp. 123–143. Springer-Verlag, Berlin/Heidelberg, (1990).